Shear induced adhesion: Contact mechanics of biological spatula-like attachment devices

Alexander Filippov, Valentin Popov, Stanislav N. Gorb

www.elsevier.com/locate/yjtbi

Shear induced adhesion: Contact mechanics of biological spatula-like attachment devices

Alexander Filippov, Valentin Popov, Stanislav N. Gorb

PII: S0022-5193(11)00075-0
DOI: doi:10.1016/j.jtbi.2011.01.049
Reference: YJTBI6361

To appear in: *Journal of Theoretical Biology*

Received date: 12 October 2010
Revised date: 30 January 2011
Accepted date: 31 January 2011

Cite this article as: Alexander Filippov, Valentin Popov and Stanislav N. Gorb, Shear induced adhesion: Contact mechanics of biological spatula-like attachment devices, *Journal of Theoretical Biology*, doi:10.1016/j.jtbi.2011.01.049

Shear induced adhesion: contact mechanics of biological spatula-like attachment devices

Alexander Filippov[a], Valentin Popov[b] and Stanislav N. Gorb[c]

[a] *Donetsk Institute for Physics and Engineering, National Academy of Science, Ukraine*

[b] *Technische Universität Berlin, Institut für Mechanik, FG Systemdynamik und Reibungsphysik, Sekr. C8-4, Raum M 122, Straße des 17. Juni 135, 10623 Berlin, v.popov@tu-berlin.de*

[c] *Department of Functional Morphology and Biomechanics, Zoological Institute of the University of Kiel, Kiel 24098, Germany, sgorb@zoologie.uni-kiel.de*

Most biological hairy adhesive systems of insects, arachnids and reptiles, involved in locomotion, rely not on flat punches on their tips, but rather on spatulate structures. Several hypotheses have been previously proposed to explain the functional importance of this particular contact geometry: (1) enhancement of adaptability to the rough substrate; (2) contact formation by shear force rather than by normal load; (3) increase of total peeling line due to using an array of multiple spatulae; (4) contact breakage by peeling off. In the present paper, we used numerical approach to study dynamics of spatulate tips during contact formation on rough substrates. The model clearly demonstrates that the contact area increases under applied shear force, especially when spatulae are misaligned prior to the contact formation. Applied shear force has an optimum describing the situation when maximal contact is formed but no slip occurs. At such equilibrium maximal adhesion can be generated. This principle manifests the crucial role of spatulate terminal elements in biological fibrillar adhesion.

Introduction

Attachment systems of insects, arachnids and reptiles have been intensively studied during the last decade (see review by Creton and Gorb, 2007), in order to reveal functional principles behind their amazing dynamical adhesive performance. Hairy (fibrillar) types of such systems consist of arrays of hairs called setae usually containing one or several levels of hierarchy (Hiller, 1968; Autumn et al., 2000; Gorb, 2001; 2005; Kim and Bhushan, 2007). Such a complexity in their structure allows them to form of a large contact area on flat and rough surfaces, thus, effecting the generation of a strong adhesion based on a combination of molecular interaction and/or capillary attractive forces (Autumn et al., 2000; Autumn and Peattie, 2002; Langer et al., 2004; Huber et al., 2005). The topmost hierarchical level of seta that is responsible for the formation of intimate contact with the substrate is not flat punch-like, but rather resembles thin film or spatula (Stork, 1980; 1983; Gorb, 1998; 2000; Persson and Gorb, 2003; Spolenak et al., 2005; Tian et al., 2006). Recently, the contact formed between an individual spatula-like terminal element and substrate was visualized on fresh pads of different animals using Cryo-SEM technique (Varenberg et al., 2010). Spatulae bear a gradient of thickness from the base to the tip of the spatula (fly: Gorb, 1998; gecko: Persson and Gorb, 2003; beetle: Eimüller et al., 2008) (Fig. 1 B, C). In contact, spatulae are aligned and orientated to the distal direction of the pad (Fig. 1 A, B).

Several hypotheses have been previously proposed to explain the functional importance of such a contact geometry: (1) enhancement of adaptability to the rough substrate (Persson and Gorb, 2003); (2) contact formation by shear force rather than by normal load (Autumn et al., 2000); (3) increase of total peeling line due to using an array of multiple spatulae (Varenberg et al., 2010); (4) contact breakage by peeling off (Gao et al., 2005). The Kendall peeling model (Kendall, 1975) was recently employed to explain the role of multiple spatulate tips in the enhancement of the total peeling line (Varenberg et al., 2010). It is well known that application of a normal force can enhance adhesion (Popov, 2010). However, for hairy

attachment systems, the adhesion force always remains smaller than the initially applied normal force (Schargott, Popov and Gorb, 2006). This would be not enough to enable walking on the ceiling. Another possibility of enhancing the adhesion force is application of a shear force. We have previously shown that applied shear force to a particular direction of the spider's spatulated setae results in an increase of real contact area (Niederegger and Gorb, 2006) (Fig. 1 e, f). Also, flies employ shear movements during contact formation by their attachment devices (Niederegger and Gorb, 2003). Previous authors revealed strong shear dependence of measured pull off force in the gecko attachment system and even called this effect "*frictional adhesion*" (Autumn et al., 2000; Autumn et al. 2006). Since the effective elastic modulus of thin plates is very small, even for relatively stiff materials such as keratin or arthropod cuticle, this geometry is of fundamental importance for adhesion on rough substrates (Persson and Gorb, 2003) due to the low deformation energy stored in the material during contact formation. We have previously shown that adhesion in such systems depends on the nature of the substrate roughness (Gorb, 2001; Peressadko and Gorb, 2004; Huber et al., 2007), and it is stronger in attachment devices containing predominantly spatulate tips (Voigt et al., 2008).

The important role of spatulate contact elements in the generation of adhesion has recently been experimentally demonstrated on artificial, bioinspired surfaces with similar geometry (Kim and Sitti, 2006; Kim et al., 2007; 2008; Murphy et al., 2007). Recent theoretical considerations supported the importance of applied shear force (pre-tension) for an increase of the peel-off force (Chen et al., 2009). However, it remains unclear how the contact on a rough substrate can be generated by shear, especially if the spatulae are initially not aligned in the plane of the substrate. In the present paper, we used a numerical approach to study the dynamics of spatulate tips during contact formation on rough substrates. The following questions were asked. (1) What is the role of the thickness gradient during contact formation? (2) Does applied shear force contribute to the enhancement of contact area on the

rough substrate. (3) Is there any optimal shear distance/force for single spatula?

Microscopical observations

To visualize setal tips, we examined attachment pads of various representatives of insects, flies, spiders, and reptiles. Insect and spider tarsi were cut off from anesthetized animals with a fine razor blade. In the case of reptiles, molted toe skin was used. Some samples were brought in contact with a glass slide by using fine forceps. The contact was formed by applying a slight shear movement, as previously described to be the natural movement in contact formation in flies (Niederegger and Gorb, 2003). Other samples were mounted on stubs, in the manner providing visualization of spatulae from their contact side. After air drying and sputter coating with gold-palladium, samples were observed in scanning electron microscope (SEM) (for details of sample preparation, see Gorb, 1998). For cryo-SEM, samples were mounted on metal holders, frozen in liquid nitrogen, and transferred to the Hitachi S-4800 cryo-SEM (Hitachi High-Technologies Corp., Tokyo, Japan) equipped with a Gatan ALTO 2500 cryo-preparation system (Gatan Inc., Abingdon, UK). The possible contamination by frozen crystals of condensed water was prevented by sublimating for 2 min (sample at -90 °C, cooler at -140 °C). After sublimation, samples were sputter-coated with gold-palladium (to a thickness of 3-6 nm) in the preparation chamber, and examined in the SEM at accelerating voltage of 3 kV at -120 °C (for details of sample preparation, see Gorb, 2006). Some samples were fixated, embedded in epoxy resin, dissected, mounted, contrasted, and observed in the transmission electron microscope (TEM) (for details of sample preparation, see Gorb, 1998).

Examples of the spatulate contact geometry of different animals are shown in Fig. 1. The SEM images demonstrate similar contact geometry of setal tips in different animal lineages. Spatulae, independent of their dimensions, make flat contact with the substrate with their free ends oriented in the distal direction (Varenberg et al., 2010) (Fig. 1 a, b). Spatulae have a gradient of thickness from distal (thinner) to the basal (thicker) part (Fig. 1 b, c)

(Eimüller et al., 2008). On rough substrates, spatulae are partially able to adapt to the surface profile (Fig. 1 b). In the non-contact state, spatulae are preferably, but not ideally, aligned (Fig. 1 d). When shear force is applied in one direction (direction depends on the species and on the site of the leg), spatulae make contact with the substrate (Fig. 1 e). When shear is applied in the opposite direction, spatulae lose the contact (Fig. 1 f).

Numerical model and discussion

To simulate shear caused adhesion in a typical spatula-like structure we appied the following model. Terminal part of the spatula is treated as a flexible elastic plate with the width (and corresponding flexural stiffness) gradually varying along the x-coordinate. The plate is brought into an initial touch with a rigid rough "ceiling" surface along a terminal line which is parallel to the y-coordinate. Generally, it is supposed to be initially inclined to the horizontal plane with a trial tilt angle α which varies in the interval $0 < \alpha < \pi/2$ from a horizontal to a vertical orientation.

Conceptual structure of the model is presented in Fig. 2, which qualitatively shows a 2-dimensional projection of the system onto the x-z-plane. It is expected that the very thin end part of the plate is flexible enough to quite easily attract to the rigid rough surface by Van der Waals force. For the sake of simplicity we simulate it by gradient of Morse potential $U_{VdW}(r) = U_o(1-\exp(-ar))^2$ with a physically reasonable amplitude $U_0 \simeq 10\ nN \cdot nm$ and the minimum located at the distance $a \simeq 1\ nm$ from the surface.

Rigid ceiling surface can be simulated by the self-affine fractal surface given by real part of $Z(x,y) = A\iint dq_x dq_y C(q)\exp(iq_x x + iq_y y + \zeta)$ with scaling spectral density. Here A is amplitude of surface roughness, i is imaginary unit, $q_{x,y}$ are Fourier components along x and y directions and ζ is a random phase. Details of the generation procedure for the profile $Z(x,y)$ have been described in a number of previous papers (see for example, Filippov and

Popov, 2007 and Popov V.L., Starcevic J., Filippov A.E., 2007). It is well accepted in the current literature (Persson and Gorb, 2003) that such presentation of the surface is suitable for a majority of physical surfaces at scale-invariant spectrum $C(q) = 1/q^{\beta}$ and value of index $\beta \approx 0.9$.

In this paper we concentrate our attention on a single spatula. Accordingly, we restrict the amplitude A of the surface profile to $A = 1\ nm$. With this amplitude the procedure generates random realizations of the rigid surface a having typical roughness up to $4\ nm$, which is typical for the considered scale.

Van der Waals attraction to the surface competes with the resistance of the spatula to bending. According to the theory of elasticity (Landau and Lifshits, 1981) elastic energy of the flexible plate is given by the following integral:

$$W_{elastic} = \frac{E}{24(1-\nu^2)} \iint dxdy h^3(x,y) \left\{ \left(\frac{\partial^2 z}{\partial x^2} + \frac{\partial^2 z}{\partial y^2} \right)^2 + 2(1-\nu) \left[\left(\frac{\partial^2 z}{\partial x \partial y} \right)^2 - \frac{\partial^2 z}{\partial x^2} \frac{\partial^2 z}{\partial y^2} \right] \right\} \quad (1)$$

where E is the Young's modulus of the plate material and ν is the Poisson ratio which is typically equal to $\nu = 1/3$. In considered systems, adhesive force is comparable to the weight of the whole animal. Thus, the gravitational force acting on the spatula is negligible. Further, due to strong internal damping in the spatula material, the system can be treated as over-damped. The over-damped dynamics of the system along vertical z coordinate is described by the equation of motion

$$\gamma \frac{\partial z(x,y)}{\partial t} = -\frac{\partial W_{elastic}[z]}{\partial z} - \frac{\partial U_{VdW}[z]}{\partial z}, \quad (2)$$

where γ is damping constant which determines a characterictic time scale of the process ($\gamma = 1$). Van der Waals bonding also produces horizontal force $F^x_{VdW} = -\partial U_{VdW}[z(x)]/\partial x$. This force competes with an external shear force F^x. When F^x exceeds the total resistance of all instantly bonded segments $\int dxdy F^x_{VdW} > |F^x|$, the whole spatula moves along the x-direction

according to the relation: $\gamma \partial x / \partial t = F^x - \int dxdy F^x_{VdW}$

A typical numerically found intermediate configuration of the system described by Eq.(2) is shown in Fig.3. The dynamic behavior leading to picture Fig.3 is as follows. The "spatula" plate is initially attached to the surface by Van der Waals force $F_{VdW} = -\frac{\partial U_{VdW}[z]}{\partial z}$ by one of its end segments. It then relaxes in the course of time to an equilibrium state in which it adheres to the surface by additional segments. The rate of attachment depends on the angle α between the plate and surface, normally being faster for smaller angles α.

If external force is nonzero $F \neq 0$, it pulls the plate to the left and competes with Van der Waals attachment F_{VdW} of the "glued" segments. If the total attachment force is stronger than the horizontal component of the external force $\int dxdy F^x_{VdW} > |F^x|$, the spatula does not slide along the x-axis. However, the part which remains unattached can rotate and approach the surface $z(x, y) \to < Z >$ (here symbol $< ... >$ denotes mean value) due to the action of the vertical component of the force $F^z > 0; F^z \sim z$. This rotation reduces mutual distances between hard and flexible surfaces and can greatly enhance the total adhesion. Generally, one can expect that a stronger shear force will cause faster attachment. However, if the shear force is too strong it can exceed the Van der Waals locking and even lead to detachment of previously attached segments. In this case, the plate will start to slip along the surface, its rotation stops and additional segments do not adhere to the ceiling. These qualitative considerations gives rise to the optimization problem: up to which extent can one vary shear force to stimulate attachment without rupturing the contact?

We have performed two sets of numerical simulations: with a fixed initial inclination angle α and varying force F and with a fixed force and varying angle. The results are summarized in Figs.4-5. The numerical experiment is organized as follows. In each experiment first a rigid surface $Z(x, y)$, with the same fractal properties, is generated as a two

dimensional array. Each array has a size of $[500,200]$ cells (corresponding to a region of $500\times200\,nm$, while the terminal part of the spatula moving against the rigid surface has the size $200\times200\,nm$. Such a size of the array is found to be large enough to provide good statistics for substantial self-averaging of the integral values (like total force, fraction of the attached segments, etc.). Now we bring one end of the plate into contact with the hard surface at some trial angle α and wait for a short period of time (about $t_0 = 2\ \mu$s in dimensional units), during which the spatula starts to adapt spontaneously to the rigid surface (at zero external force $F_{t<t_0} = 0$). At $t = t_0$ we "turn on" the pulling. The process is continued up to the maximal time $t_{\max} = 10\ ms$, which corresponds to the observed time for contact formation of the gecko toe (Gao et al. , 2005).

Subplot (a) in Fig. 4. shows how a part of the plate contacting with the rigid surface (normalized to its total area) grows with time at different values of the pulling force F at fixed trial inclination angle $\alpha = const$ (here we use a representative intermediate angle $\alpha = \frac{\pi}{5}$). One can see, that different random realizations of the substrate surface $Z(x,y)$ manifest themselves only in small deviations (and sometimes mutual intersections) of the subsequent solutions in Fig.4 but do not affect the general monotonous trend. This observation is important to be sure that the obtained results are representative.

As expected, the higher force F leads to a faster decrease of the inclination angle. If the force is smaller than some critical value for detachment $F < F_{crit} \approx 20\,nN$, which is in the range of forces previously experimentally measured for single gecko spatulae (Huber et al., 2005a), then the plate gradually tends to a horizontal orientation for $t \to \infty$. When the force approaches the critical value F_{crit} it becomes capable of breaking some of the already attached bonds and to slightly shift the plate in a horizontal direction. Corresponding small horizontal displacements $\delta x = x - x_0$ of the system from its initial position x_0 are clearly seen in the

subplot (b) (curves 3-6), where time dependencies of the shift $\delta x(t)$ are presented for different forces.. The arrows in both subplots show how the time dependencies change with increasing external force F. Finally, if the force exceeds a threshold F_{crit} (curves 1 and 2) it completely breaks the initial attachment and causes permanent sliding of the plate. In this regime the plate does not rotate and does not further approach the horizontal orientation, thus not leading to any increase of adhesion. It is natural that in a biological system the animal cannot control the state (attachment and orientation) of each individual spatula, but presumably can monitor a total resistance force of the entire spatulla array, keeping it close to but not exceeding the critical value.

As mentioned above, the critical force F_{crit} depends on an initially attached area and thus on a trial inclination of a particular spatula. It is important to study variations of the time-depending scenarios at changes of the initial angle α. The results of this study are summarized in Fig.5, where time dependencies of the attached fraction calculated at fixed value of the pulling force $F = 10\,nN$ are shown for different trial angles α, which is varied with a constant step from almost horizontal to almost vertical orientation: $0.05 \cdot \frac{\pi}{2} \le \alpha \le 0.95 \cdot \frac{\pi}{2}$. Two limiting cases of this interval are presented by the curves 1 and 11, respectively. The arrow shows how a time dependant scenario varies, increasing the angle in the interval $0.05 \cdot \frac{\pi}{2} < \alpha < 0.95 \cdot \frac{\pi}{2}$. It is clearly seen that the shear enforces the attachment process, even at very acute angles (curves 1-3), when the fraction of the attached segments quickly spontaneously grows even at $t < t_0$.

Implications to biological systems

Spatulate contact geometry occurs widely in biological attachment devices related to locomotion in contrast to mushroom shaped contact geometry adapted to long-term

attachment (Gorb and Varenberg, 2007). Locomotory function requires rapid and reliable contact formation and breakage, which can be achieved by applied shear force (formation) and peeling (breakage) (Autumn et al., 2000; 2006; Niederegger and Gorb, 2003; Gao et al., 2005; Tian et al., 2006; Chen et al., 2009).

Recently, Chen et al., (2009) have generalized Kendall's (1975) model of an elastic film adhering on a substrate by incorporating the effect of a pre-tension in the film. This has allowed authors to investigate the effect of the pre-tension on the orientation dependent adhesion strength of a spatula pad on substrate. The main result of this study was that pre-tension can significantly enlarge the peel-off force at small peeling angles while decreasing it at large peeling angles, resulting in strong reversible adhesion.

Our study demonstrates three additional functional aspects of spatulate geometry on adhesion. The first one is that contact area grows on smooth and rough surfaces under applied shear force, especially when spatulae are misaligned prior to contact formation, which is the case in the gecko system. The second important finding is that applied shear force has an optimum, which describes the situation when the maximal contact is formedbut no slip occurs. At such equilibrium maximal adhesion can be generated. The third interesting observation is that, due to the thickness gradient, the initial contact is formed by the spatula tip. This initial contact, together with applied shear, results in a further increase of the contact area which is responsible for stronger adhesion. These principles manifest the critical role of spatulate terminal elements in biological fibrillar adhesion.

However, even when the minimum free-energy state corresponds to complete contact, the elastic plate may be trapped in a metastable state because of friction. In this case, because the kinetic friction is smaller than the static friction, sliding or vibrating the plate may increase the contact area (Niederegger and Gorb, 2006). This effect is known experimentally: by sliding of spatulae for a short distance the contact area (Niederegger and Gorb, 2006) and friction/adhesion increase (Autumn et al., 2000; 2006).

Conclusions

Contact formation, not by applying normal loadbut rather by shear force, is one of the possible reasons why most biological, hairy, locomotory attachment systems rely on spatulate structures. Shear force applied to spatulae, initially oriented at various angles, results in the proper alignment of the spatulae and an increase of the contact area to smooth and rough substrates. This principle generalizes the critical role of terminal elements in fibrillar adhesion. Finally, we can suggest that bio-inspired adhesives based on spatulate geometry has to be actuated according to the scheme preload-shear-peel, in contrast to mushroom shaped geometry of terminal tips (Varenberg and Gorb, 2007).

Acknowledgements

V. Kastner (Max-Planck Institute for Metals Research, Stuttgart, Germany) provided linguistic corrections of the manuscript. This study was supported by the Federal Ministry of Education and Research, Germany (project BMBF Biona 01RB0802A) to S.G. and the Deutsche Forschungsgemeinschaft (A.F.).

References

Autumn, K., Dittmore, A., Santos, D., Spenko, M. and Cutkosky, M. (2006) Frictional adhesion: a new angle on gecko attachment. Journal of Experimental Biology 209: 3569-3579.

Autumn, K., Liang, Y. A., Hsieh, S. T., Zesch, W., Chan, W. P., Kenny, T. W., Fearing, R. and Full, R. J. (2000) Adhesive force of a single gecko foot-hair. Nature 405: 681-685.

Autumn, K. and Peattie, A.M. (2002) Mechanisms of adhesion in geckos. Integr. Comp. Biol. 42: 1081-1090.

Chen, B., Wu, P.D., Gao H. (2009) Pre-tension generates strongly reversible adhesion of a spatula pad on a substrate. J.R. Soc. Interface, 6, 529-537.

Creton, C. and Gorb, S.N. (2007) Sticky feet: from animals to materials. MRS Bulletin 32: 466-472.

Eimüller, T., Guttmann, P., and S. N. Gorb (2008) Terminal contact elements of insect attachment devices studied by transmission X-ray microscopy. Journal of Experimental Biology 211: 1958-1963.

Filippov A.E. and Popov V.L. (2007) Fractal Tomlinson model for mesoscopic friction: From microscopic velocity-dependent damping to macroscopic Coulomb friction. Phys.Rev. E75, 027103.

Filippov A.E. and Popov V. (2007) Flexible tissue with fibres interacting with an adhesive surface. J. Phys.: Condens. Matter 19: 096012 (10pp).

Gao, H., Wang, X., Yao, H., Gorb, S.N. and Arzt, E. (2005) Mechanics of hierarchical adhesion structures of geckos. Mechanics of Materials 37: 275-285.

Gorb, S.N. (1998) The design of the fly adhesive pad: distal tenent setae are adapted to the delivery of an adhesive secretion. Proc. Roy. Soc. London B 265: 747-752

Gorb, S.N. (2001) *Attachment devices of insect cuticle*, Kluwer Academic Publishers,

Dordrecht.

Gorb, S. N. (2005) Uncovering insect stickiness: structure and properties of hairy attachment devices. American Entomologist 51 (1): 31-35.

Gorb, S.N. (2006) Fly microdroplets viewed big: a Cryo-SEM approach. Microscopy today 14 (5): 38-39.

Gorb, S.N. and Varenberg, M. (2007) Mushroom-shaped geometry of contact elements in biological adhesive systems. J. Adhesion Sci. Technol. 21 (12-13): 1175-1183.

Hiller, U. (1968) Untersuchungen zum Feinbau und zur Funktion der Haftborsten von Reptilien. Z. Morphol. Tiere 62: 307-362.

Huber, G., Gorb, S.N., Spolenak, R. and Arzt, E. (2005a) Resolving the nanoscale adhesion of individual gecko spatulae by atomic force microscopy. Biol. Lett. 1: 2-4.

Huber, G., Gorb, S.N., Hosoda, N., Spolenak, R. and Arzt, E. (2007) Influence of surface roughness on gecko adhesion. Acta Biomaterialia 3: 607-610.

Huber, G., Mantz, H., Spolenak, R., Mecke, K., Jacobs, K., Gorb, S.N. and Arzt, E. (2005b) Evidence for capillarity contributions to gecko adhesion from single spatula nanomechanical measurements. PNAS 102 (45): 16293-16296.

Kendall, K. (1975) Thin-film peeling--the elastic term. J. Phys. D Appl. Phys., 8: 1449-1452.

Kim, S., Aksak, B. and Sitti M. (2007) Enhanced friction of elastomer microfiber adhesives with spatulate tips. Appl. Phys. Lett. 91, 221913.

Kim, S. and Sitti, M. (2006) Biologically inspired polymer microfibers with spatulate tips as repeatable fibrillar adhesives. Applied Physics Letters 89, no. 261911.

Kim, S., Sitti, M., Jang, J-H., Thomas, E.L. (2008) Fabrication of bio-inspired elastomer nanofiber arrays with spatulate tips using notching effect. IEEE Nano, pp. 780-782.

Kim T.W. and Bhushan B. (2007) Adhesion analysis of multi-level hierarchical attachment system contacting with a rough surface. Journal of Adhesion Science and Technology. 21(1): 1-20.

Landau L.D. and Lifshits E.M. (1981) Theory of elasticity, Pergamon Press, Oxford, 2 edition, 176 pp.

Langer, M.G. Ruppersberg, J.P. and Gorb, S.N. (2004) Adhesion forces measured at the level of a terminal plate of the fly's seta. P. Roy. Soc. Lond. B, 271:2209-2215.

Murphy, M.P., Aksak, B., Sitti, M. (2007) Adhesion and anisotropic friction enhancements of angled heterogeneous micro-fiber arrays with spherical and spatula tips. Journal of Adhesion Science and Technology 21(12-13): 1281-1296.

Niederegger, S. and Gorb, S.N. (2003) Tarsal movements in flies during leg attachment and detachment on a smoothe substrate. J. Insect Physiol. 49: 611-620.

Niederegger, S. and Gorb, S.N. (2006) Friction and adhesion in the tarsal and metatarsal scopulae of spiders. J. Comp. Physiol. A 192: 1223-1232.

Peressadko, A. and Gorb, S.N. (2004) Surface profile and friction force generated by insects. In: Fortschritt-Berichte VDI. Eds: Boblan, I. and Bannasch, R., VDI Verlag, Düsseldorf. 249(15): 257-263.

Persson, B. N. J. and Gorb, S.N. (2003) The effect of surface roughness on the adhesion of elastic plates with application to biological systems. Journal of Chemical Physics 119 (21): 11437-11444.

Popov V.L. (2010) Contact Mechanics and Friction. Physical Principles and Applications. – Springer-Verlag, 362 pp.

Popov V.L., Starcevic J., Filippov A.E.(2007) Reconstruction of potential from dynamic experiments. - Phys. Rev. E, 75: 066104 (6 pp).

Schargott M, Popov V., Gorb S. (2006) Spring model of biological attachment pads. Journal of theoretical Biology 243: 48-53.

Spolenak, R., Gorb, S.N., Gao, H. and Arzt, E. (2005) Effects of contact shape on the scaling of biological attachments Proc. R. Soc. A 461: 305-319.

Stork, N.E. (1980) A scanning electron microscope study of tarsal adhesive setae in the Coleoptera. Zool. J. Linn. Soc. 68: 173-306.

Stork, N.E. (1983) The adherence of beetle tarsal setae to glass. J. Nat. Hist. 17: 583-597.

Tian, Y., Pesika, N., Zeng, H., Rosenberg, K., Zhao, B., McGuiggan, P., Autumn, K. and Israelachvili, J. (2006) Adhesion and friction in gecko attachment and detachment. PNAS 103 (51): 19320-19325.

Varenberg, M. and Gorb, S.N. (2008) Shearing of fibrillar adhesive microstructure: friction and shear-related changes in pull-off force. Journal of the Royal Society Interface 4: 721-725.

Varenberg, M., Pugno, N.M. and Gorb, S.N. (2010) Spatulate structures in biological fibrillar adhesion. Soft Matter 6: 3269-3272.

Voigt, D., Schuppert, J.M., Dattinger, S. and Gorb, S.N. (2008) Sexual dimorphism in the attachment ability of the Colorado potato beetle *Leptinotarsa decemlineata* (Coleoptera: Chrysomelidae) to rough substrates. J. Insect Physiol. 54: 765-776.

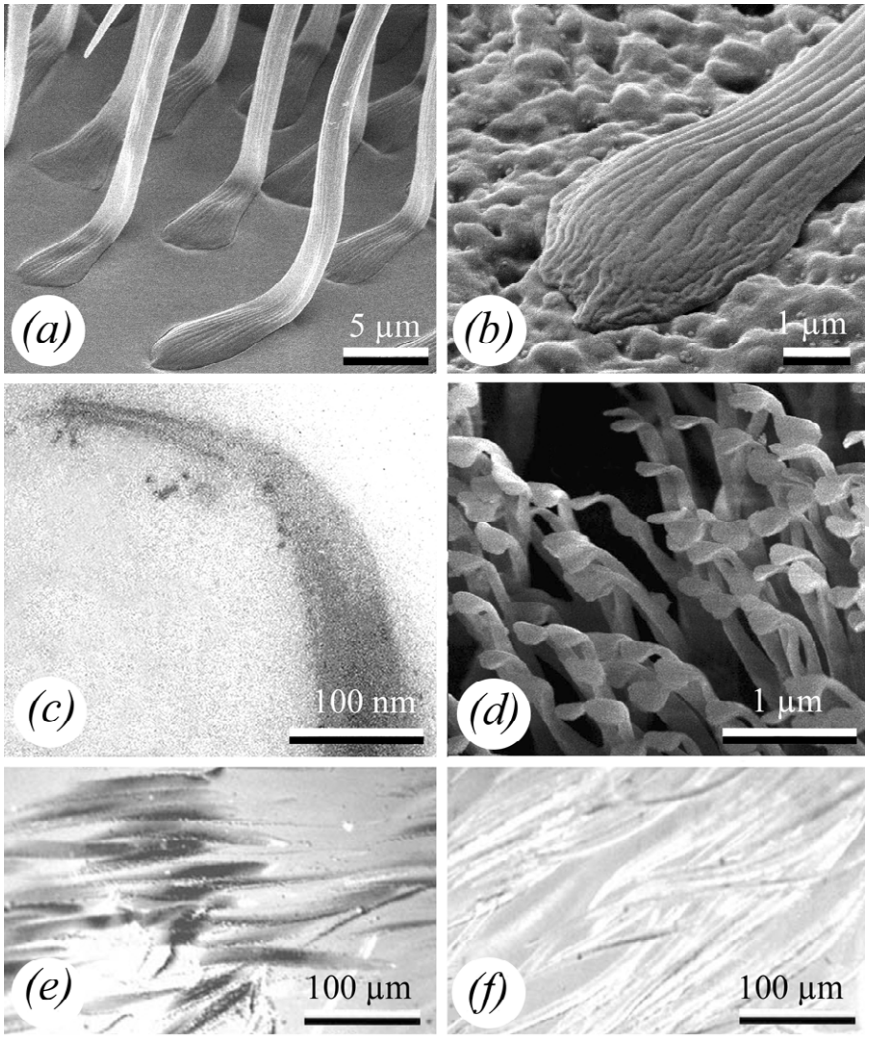

Fig. 1. Light microscopy (*e, f*), Cryo-SEM (*d*), SEM (*a, b*), and TEM (*c*) images of spatula-shaped thin-film terminal elements in hairy attachment pads of various animals. *(a)* Spatulae of the beetle *Gastrophysa viridula* in contact with the flat substrate. *(b)* Single spatula of the same species in contact with substrate having average asperity dimension in the range of 300 nm. *(c)* Longitudinal section of the single spatula of *Gekko gecko*. *(d)* Spatulae of *G. gecko*. *(e, f)* Setae of the spider *Cupiennius salei* in the reflection light microscope during distal *(e)* and proximal *(f)* sliding on a glass substrate (black areas correspond to the sites of contact between spatulae and glass surface).

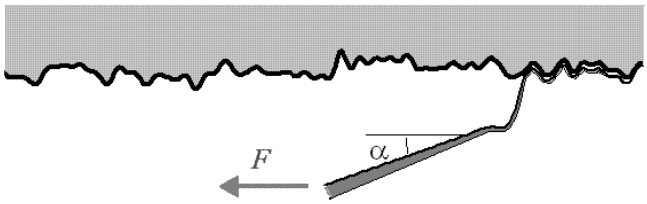

Fig. 2. Conceptual structure of the numerical model. We consider a terminal part of the "spatula" which is modeled by an elastic plate with variable thickness. It is brought into contact with the rough rigid surface at an initial inclination angle α and pulled in a horizontal direction by an external force F .

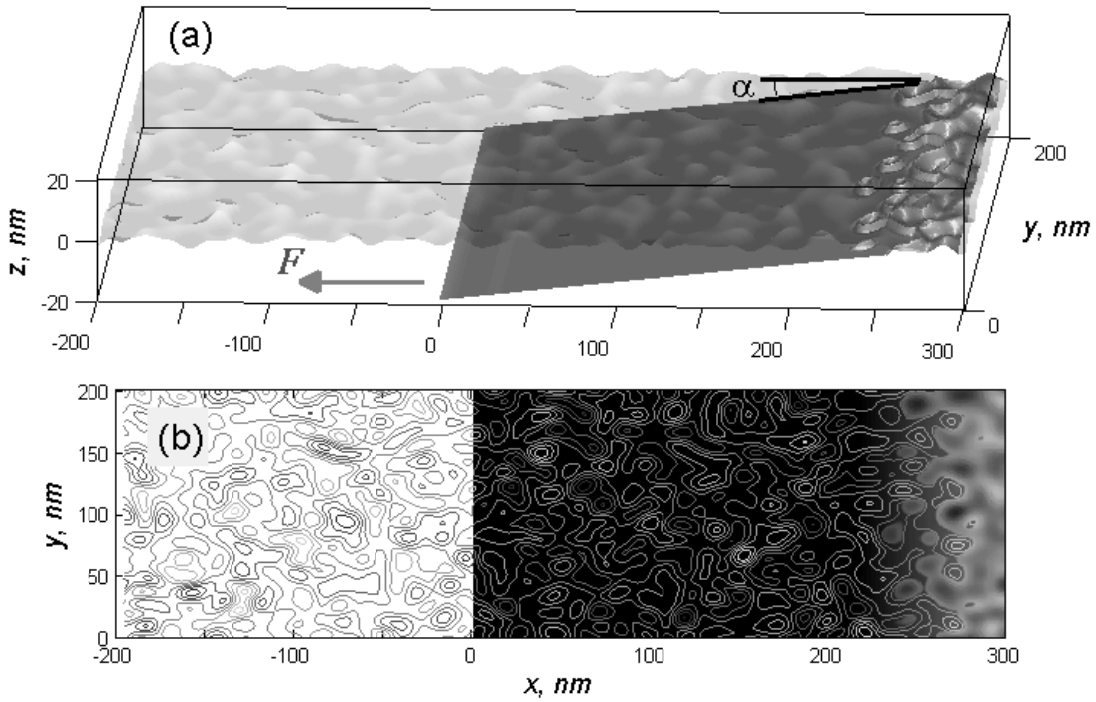

Fig. 3. Typical 3-dimensional configuration of the elastic plate found at an intermediate stage of motion (a). Rigid ceiling is shown by semi-transparent upper surface in the picture. Instant configuration of the flexible surface is presented by the gray-scale map (darker color corresponds to deeper values of z-coordinate). The picture is completed by a contour plot of the rough surface (b) where instant contact areas shown by the gray-scale map are seen directly. See two videos as electronic supplementary material.

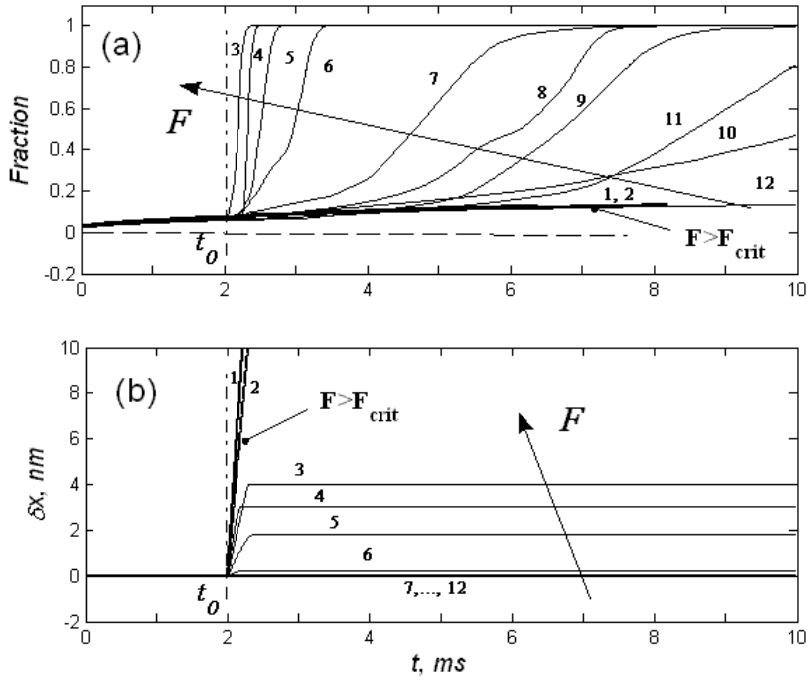

Fig. 4. Time dependencies of the attached fraction (contacting part of the plate normalized to its total area) calculated at different values of the pulling force (a) and corresponding drift δx of the attached end (b). The arrows in both subplots mark the tendencies in fraction and drift changes at increase of the force F. Bold curves 1 and 2 correspond to the forces $F = 22\,nN$ and $F = 20\,nN \geq F_{crit}$ higher than critical value F_{crit}, which is sufficient to rupture initial attachment and cause permanent slip of the plate. Other curves 3-12 correspond to the forces uniformly decreasing inside the interval $0 < F < F_{crit}$. All the dependencies are typical for an intermediate trial angle α (and obtained for a definiteness at fixed $\alpha = 0.2\pi$).

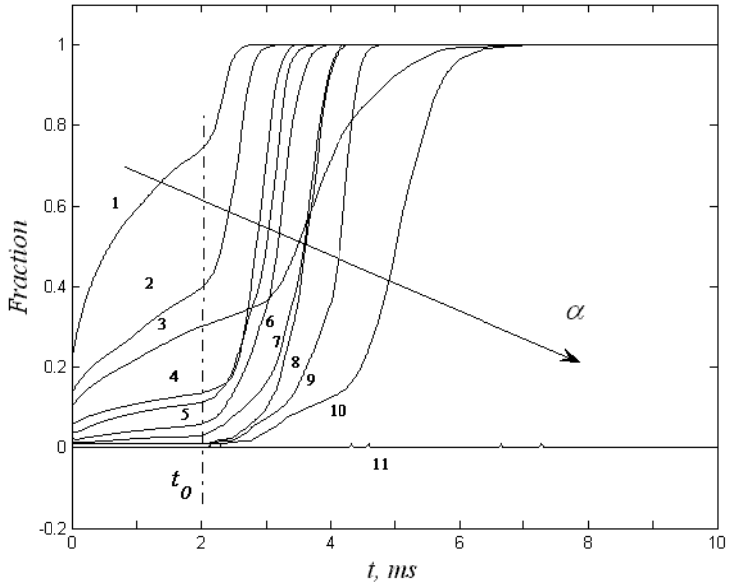

Fig. 5. Time dependencies of the attached fraction calculated at fixed value of the pulling force $F = 10\,nm$ and trial inclination angle which is gradually varied between almost horizontal and vertical orientations: $0.05 \cdot \frac{\pi}{2} \le \alpha \le 0.95 \cdot \frac{\pi}{2}$. The curves 1 and 11 correspond to the limiting cases of this interval, respectively. The arrow marks a tendency in fraction decrease at angle growth.